International Forum on Aeroelasticity and Structural Dynamics
IFASD 2017
25-28 June 2017 Como, Italy

VALIDATION AND EVALUATION OF A NONLINEAR AEROELASTIC FRAMEWORK USING FLIGHT TEST DATA

F. Afonso[1], J. Vale[1], É. Oliveira[1], F. Lau[1], F. Moreira[2], J. Marra[2], A. Meinicke[2], M. Pedras[2], O. Mello[2], J. Richards[3], W. Brussow[3], S. Warwick[3], M. Brás[3], A. Suleman[3]

[1]IDMEC, Instituto Superior Técnico, Universidade de Lisboa
Av. Rovisco Pais, 1049-001 Lisbon, Portugal

[2]EMBRAER S.A.
Av. Brigadeiro Faria Lima, 2170, São José dos Campos, São Paulo 12227-901, Brazil

[3]Department of Mechanical Engineering, University of Victoria
PO Box 1700, Stn. CSC, Victoria, British Columbia, V8W 2Y2, Canada
suleman@uvic.ca

Keywords: flexible wing, nonlinear aeroelasticity, fluid-structure interaction, experimental aeroelasticity

Abstract: One of the main concerns in the design of high aspect ratio wings is the constant change in the aerodynamic and inertial properties during flight which consequently affects its performance. To account for the structural flexibility in the preliminary design stage and adequately explore the design space, an aeroelastic framework that considers the fluid-structure interaction is employed. There are some aeroelastic frameworks specially developed to study this type of wings, although the experimental data required to evaluate and validate these frameworks is scarce, particularly in what concerns flight tests. In this work, the experimental data from the ground vibration tests, static tests and flight tests carried out for a highly flexible unmanned flight test demonstrators are used to evaluate and validate both the ASWING and an in-house nonlinear aeroelastic frameworks.

1 INTRODUCTION

In view of the current green aviation initiatives and requirements, the interest in High Aspect-Ratio Wings (HARWs) is growing for application in transport aircraft. High aspect-ratio wings allow higher lift to drag ratios. On the other hand, in order to design structural efficient airframes, these designs exhibit higher deflections under normal flight conditions than conventional aircraft. By increasing the wing structure's flexibility, geometric nonlinearities may appear causing a change in the dynamic behavior of the wing, which generally degrades its aeroelastic behavior. Reported effects include reducing the flutter speed (in its classic form corresponds to a coupling between two elastic modes) [1–3], changing the limit cycle oscillation (LCO) onset [3, 4], modifying the dynamic response [5], high sensibility to disturbances (*e.g.* gusts) [6], changes in flight dynamic behavior [1, 7, 8] and the coupling of a rigid body mode with an elastic mode (known in the literature as body-freedom flutter) [9, 10].

Several frameworks (*e.g.* ASWING [11], NATASHA [7], UM/NAST [6, 8, 10], NANSI [12] and SHARP [13]) have been developed to study this type of very flexible wings allowing for:

computing steady and unsteady aeroelastic responses; stability analyses; flight dynamic simulations which can include disturbances (usually in the form gust profiles); and flutter boundary predictions. These frameworks are normally benchmarked with existing experimental wind tunnel data and/or numerical simulations. Although, for accurately assessing the impact of wing's flexibility on the flight dynamics one requires flight test data, which is scarce in the open literature. Recent efforts have been made by Cesnik and his co-workers towards the goal of providing flight test data of a very flexible aircraft to validate these frameworks [14].

In this work, the data from the flight test campaign of a highly flexible Unmanned Air Vehicle (UAV) has been processed and used to validate an in-house nonlinear aeroelastic framework [15, 16] and ASWING [11]. The UAV has a wing aspect-ratio of just 13, and its wing frame was designed such that it reaches large deformations at low subsonic flight conditions (the airspeed in the flight tests was always lower than 30 m/s). The highly flexible aircraft planform allows to validate and evaluate the effects of geometric nonlinearities on the aeroelastic behavior and flight dynamics of HARWs. Experimental data includes results from ground vibration tests, static tests and flight tests and it is be used to compare with the modal, nonlinear static elastic and nonlinear unsteady aeroelastic solvers, respectively.

2 AEROELASTIC FRAMEWORK

To study the performance of aircraft with highly flexible wing structures, a nonlinear aeroelastic framework has been developed in-house. This tool allows to perform nonlinear aeroelastic analyses in the time domain with both constrained and unconstrained flight simulation capabilities [15, 16]. The code was implemented in C++ and is composed of 5 modules: aeroelastic, aerodynamic (3D panel method with viscous and compressibility corrections), structural (condensed 3D nonlinear beam model), propulsion (electric powered propeller) and payload distribution. The aeroelastic module coordinates the remaining modules through a Fluid-Structure Interaction (FSI) algorithm that can run both steady and dynamic analyses. This FSI algorithm was defined such that the disciplines are individually solved and the coupled solution only progresses if convergence between disciplines is reached. Linear and nonlinear aeroelastic analyses are allowed. The nonlinearities are only geometrical and are accounted for in the structural solver and transferred to the aerodynamic solver by generating a different aerodynamic mesh at each load step. A description of this in-house framework steady and unsteady formulations is provided in [16] and [15], respectively. The aerodynamic, structural and aeroelastic models were compared with available (numerical and in some cases experimental) data in the literature presenting good results for the analyses carried out: steady aerodynamics; nonlinear static and dynamic analyses (structural); free-vibrations; flutter boundary calculation.

3 AIRCRAFT MODEL

An aircraft platform developed in-house was used for this work. In order to allow studying the effects of flexibility on the flight dynamics, the wing was specially designed such that the frequency of the first flap bending mode becomes closer to the short period frequency as the airspeed increases. This wing has an aspect-ratio of 13.22, an area of 0.96 m^2 and a mean aerodynamic chord of 0.27 m while the aircraft weight is 19.8 kg.

The structural model in both aeroelastic framework and ASWING was defined based on the cross-sectional data (bending and torsional stiffness values) and material properties defined in the NASTRAN model after updating it with experimental results. Non-structural weights

such as batteries and payload were considered as mass points rigidly linked to the structure, in the aeroelastic framework the inertial properties of these weights are computed in the payload module. For the aerodynamics, 3D panel code and vortice lattice method were used in the in-house framework and ASWING, respectively. An electric propulsive system was defined in the aeroelastic framework, where a semi-empirical electric motor model based on experimental data was employed.

4 EXPERIMENTAL WORK DESCRIPTION

As aforementioned the wing structure was designed to be very flexible such that its first elastic mode (flap bending) couples with the short period within a reachable airspeed. Preliminary studies were carried out in ASWING to evaluate the aeroelastic behavior of different structures and provide valuable guidelines for the wing design in what concerns to the bending and torsional stiffness values. After selecting a suitable bending and torsional stiffness, a wing structure was designed in CAD (Computer-Aided Design) software and built considering the in-house experience.

Before performing the flight tests, several tests were made to characterize the structure and update the computational models. First the inertia properties were determined using bifilar pendulum tests, followed by static load tests and ground vibration tests. Also, control surface calibration, pre-flight and non-instrumented flight tests were carried out to ensure that aircraft was ready to fly.

The airworthiness of the flexible aircraft was evaluated for different flight control instructions applied to the elevator, ailerons, flaperon, rudder and throttle.

5 FRAMEWORK EVALUATION AND VALIDATION

A NASTRAN model of the structure was defined and integrated in an optimization problem to achieve the same dynamic behavior captured in the experiments after a few manual adjustments, which include the definition of the mass points (*e.g.* electric motor, batteries and payload). The resulting model was then used for modeling the wing in both ASWING and aeroelastic (in-house) framework. For this task, the cross-sectional dimensions, material properties, mass points and joints' stiffness values were parametrized in the NASTRAN model and set as design variables for the optimization. The objective function comprises the relative errors of natural frequencies, mode shapes (in the form of Modal Assurance Criteria) and static deflections in reference to the collected data. Overall mass and center of gravity (cg) location were set as constraints for this optimization problem.

With the resulting NASTRAN model (values for bending and torsional stiffness, mass points, material properties and joints' stiffness) that has converged with a small error, the ASWING and aeroelastic framework models were defined. Herein, the results from the experiments, aeroelastic framework and ASWING are compared for 4 different analyses: inertia properties; static; natural frequencies; steady non-linear elastic. The experimental flight test data is used to compare the results obtained with ASWING for unsteady and unconstrained aeroelastic analysis.

5.1 Inertia Properties

Since the data from the bifilar pendulum tests was already used to generate the updated NASTRAN model, which was then employed to define the aeroelastic models (in both ASWING

and in-house framework), the differences between experimental and computational results are expected to be low. This was verified (see Table 1) for the cg location (x_{cg}, y_{cg}, z_{cg}), overall mass and inertia moments (computed with reference to the aircraft cg) with errors lower than 5.09%, except for the cross product of inertia I_{xz} which was predicted to be much higher in the computational models than in the experiment. The reason for this discrepancy is due to the fact that the inertia moments were not accounted for in the computational model update (*i.e.* optimization problem).

	Framework	ASWING	Experimental	Difference 1	Difference 2
x_{cg}	0.6634 m	0.6635 m	0.6653 m	0.01%	0.28%
y_{cg}	0.0000 m	0.0000 m	0.0000 m	0%	0%
z_{cg}	0.0619 m	0.0624 m	0.0652 m	0.85%	5.09%
Mass	19.98 kg	20.10 kg	19.80 kg	0.61%	0.89%
I_{xx}	3.3243 kg.m^2	3.4187 kg.m^2	3.4250 kg.m^2	2.75%	2.94%
I_{yy}	3.8077 kg.m^2	3.8130 kg.m^2	3.8640 kg.m^2	0.49%	1.46%
I_{zz}	6.3842 kg.m^2	6.4813 kg.m^2	6.5270 kg.m^2	1.00%	2.19%
I_{xy}	0.0000 kg.m^2	0.0000 kg.m^2	0.0000 kg.m^2	0%	0%
I_{yz}	0.0000 kg.m^2	0.0000 kg.m^2	0.0000 kg.m^2	0%	0%
I_{xz}	0.3376 kg.m^2	0.3454 kg.m^2	0.0060 kg.m^2	1.70%	5525.87%

Table 1: Inertial properties of the aircraft in the aeroelastic framework model compared with the ASWING (Difference 1) and experimental data (Difference 2). The cg location is in reference to the aircraft nose; and the inertia moments were taken about the cg location.

5.2 Static Tests

Three experimental static load tests were performed, although only a symmetric out of plane bending test was employed for the computational model update. Thus, only the data regarding this static test case is shown. This test case consisted in applying a vertical load at points (676.01 mm; $\pm$943.57 mm; 171.203 mm) with a magnitude varying from 0 N to 78 N. Deflections at different spanwise wing locations were used to compare the experimental and computational wing deflections. In Table 2 the vertical displacement at two different spanwise positions are shown, from which one can observe that the differences between framework and experimental results are small.

Spanwise position	Framework	Experimental	Difference
0.864 m	0.1006 m	0.1020 m	1.40%
1.686 m	0.2318 m	0.2445 m	5.18%

Table 2: Vertical wing displacement in different spanwise positions when subjected to a bending moment.

5.3 Ground Vibration Tests

The ground vibration tests were conducted with two different boundary conditions yielding two sets of modal parameters (natural frequencies, damping factors and mode shapes). These conditions were simulated in the aeroelastic tools and compared with the experimental results.

Firstly, the main wing without body and empennage was cantilevered at the wing saddle (joint between wing and fuselage) simulating a fixed-free boundary condition. The natural frequencies corresponding to the first, second and third flap bending, first chord bending and first torsion modes are shown in Table 3. The relative errors between the aeroelastic framework and

ASWING are lower than 8.31% and the discrepancy was found to increase as the frequency increase. For the comparison between the aeroelastic framework and experimental data, the relative errors are smaller than 6.74%, being higher for the flap bending vibration modes than for the chord bending and torsion vibration modes.

Mode	Framework	ASWING	Experimental	Difference 1	Difference 2
1st Flap	2.72 Hz	2.72 Hz	2.89 Hz	0.06%	6.02%
1st Chord	12.6 Hz	12.5 Hz	12.9 Hz	0.63%	2.22%
2nd Flap	16.6 Hz	17.3 Hz	17.8 Hz	4.29%	6.74%
1st Torsion	36.9 Hz	39.3 Hz	37.4 Hz	6.18%	1.29%
3rd Flap	52.9 Hz	57.8 Hz	55.9 Hz	8.31%	5.40%

Table 3: First natural frequencies of the cantilevered wing in the aeroelastic framework model compared with the ASWING (Difference 1) and experimental data (Difference 2).

For the second test, the entire aircraft was suspended from bungees to simulate a free-free boundary condition. The same mode shapes as on the previous case were selected for comparison. Regarding the comparison between in-house aeroelastic framework and ASWING, the same trend was observed: the relative error increase with the frequency value increase, achieving a maximum of 8.80% for the highest frequency vibration mode that was compared. From the comparison between experimental data and aeroelastic framework, one can notice that the relative errors are smaller than 5.70% for the considered vibration modes.

Mode	Framework	ASWING	Experimental	Difference 1	Difference 2
1st Flap	2.87 Hz	2.93 Hz	3.04 Hz	2.01%	5.70%
1st Chord	13.2 Hz	13.5 Hz	12.9 Hz	2.05%	2.38%
2nd Flap	17.1 Hz	17.5 Hz	17.9 Hz	2.32%	4.71%
1st Torsion	37.3 Hz	39.4 Hz	37.7 Hz	5.44%	1.06%
3rd Flap	53.3 Hz	58.5 Hz	54.1 Hz	8.80%	1.46%

Table 4: First natural frequencies of the free aircraft in the aeroelastic framework model compared with the ASWING (Difference 1) and experimental data (Difference 2).

5.4 Flight Tests

Flight tests were conducted in order to compare the experimental data obtained from flights with prescribed control surfaces disturbances with data from aeroelastic simulations. The aeroelastic simulations were performed only with ASWING. Three different flight tests with three different control surfaces disturbances were performed, namely: elevator doublet; aileron doublet and ruder doublet. Figure 1 shows the control surfaces' deflections variation with time.

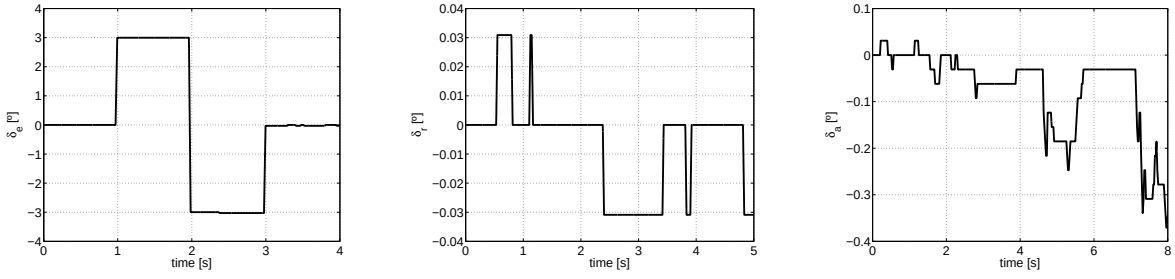

(a) Elevator (b) Rudder (c) Aileron

Figure 1: Time variation of the doublets imposed to the elevator, rudder and aileron control surfaces.

The results for the linear velocities, altitude, angle of attack, side-slip angle, angular velocity and Euler angles are shown in Figures 2, 3 4 for both experimental and ASWING nonlinear aeroelastic analysis data.

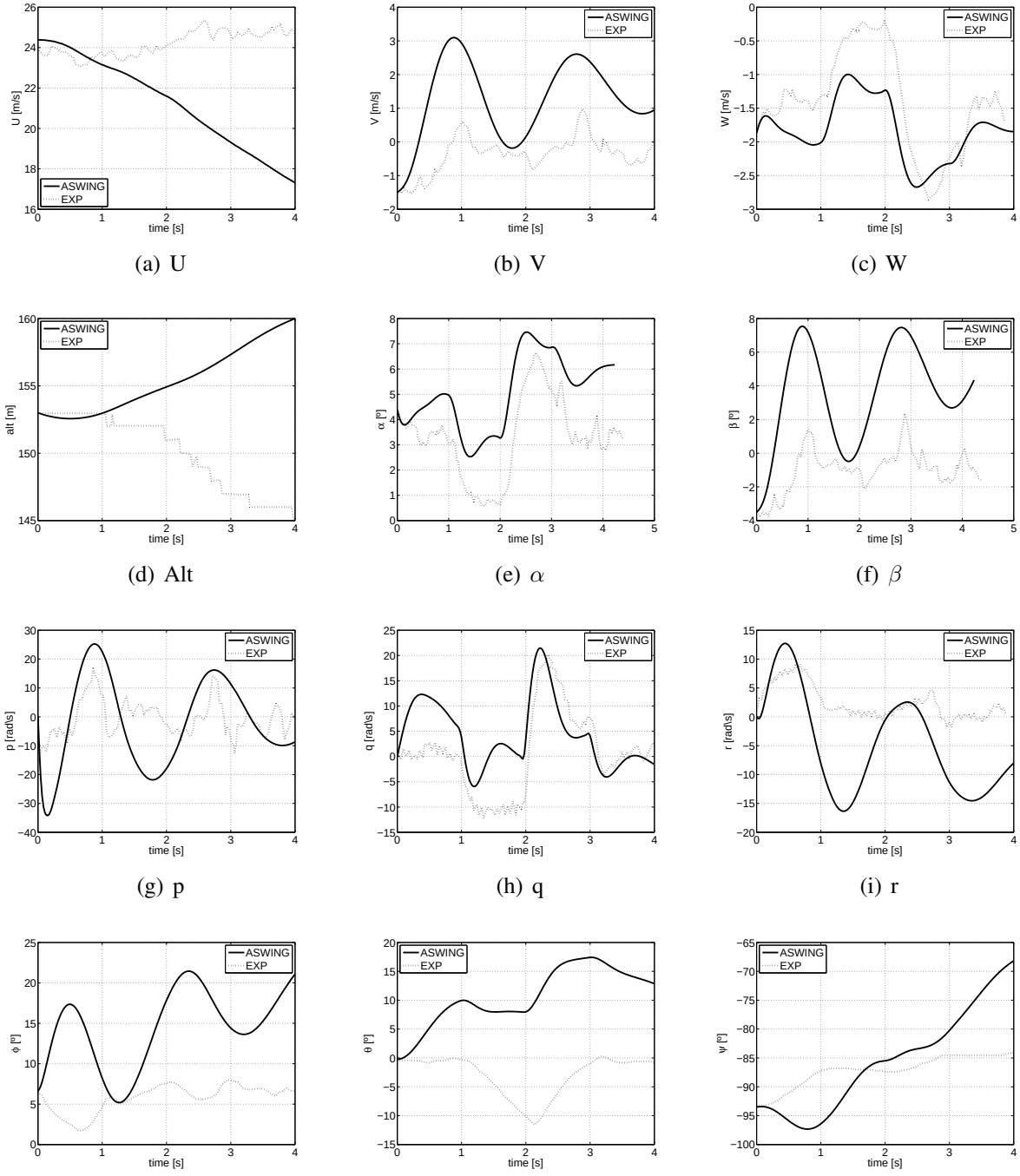

(a) U (b) V (c) W

(d) Alt (e) α (f) β

(g) p (h) q (i) r

(j) ϕ (k) θ (l) ψ

Figure 2: Dynamic response of the aircraft to an elevator doublet for linear velocities (U, V, W), altitude (alt), angle of attack (α), side-slip angle (β), angular velocities (p, q, r) and Euler angles (ϕ, θ, ψ).

Several observations can be made about the results. The first observation is that the effect of the doublets can be noticed in the experimental data, particularly in the angular rates which are most affected by the prescribed doublet. Thus, one can observe the changes in the pith rate when the elevator doublet is prescribed and the changes in roll and yaw rates when aileron and rudder doublets are prescribed. The second observation is that the ASWING results do not match

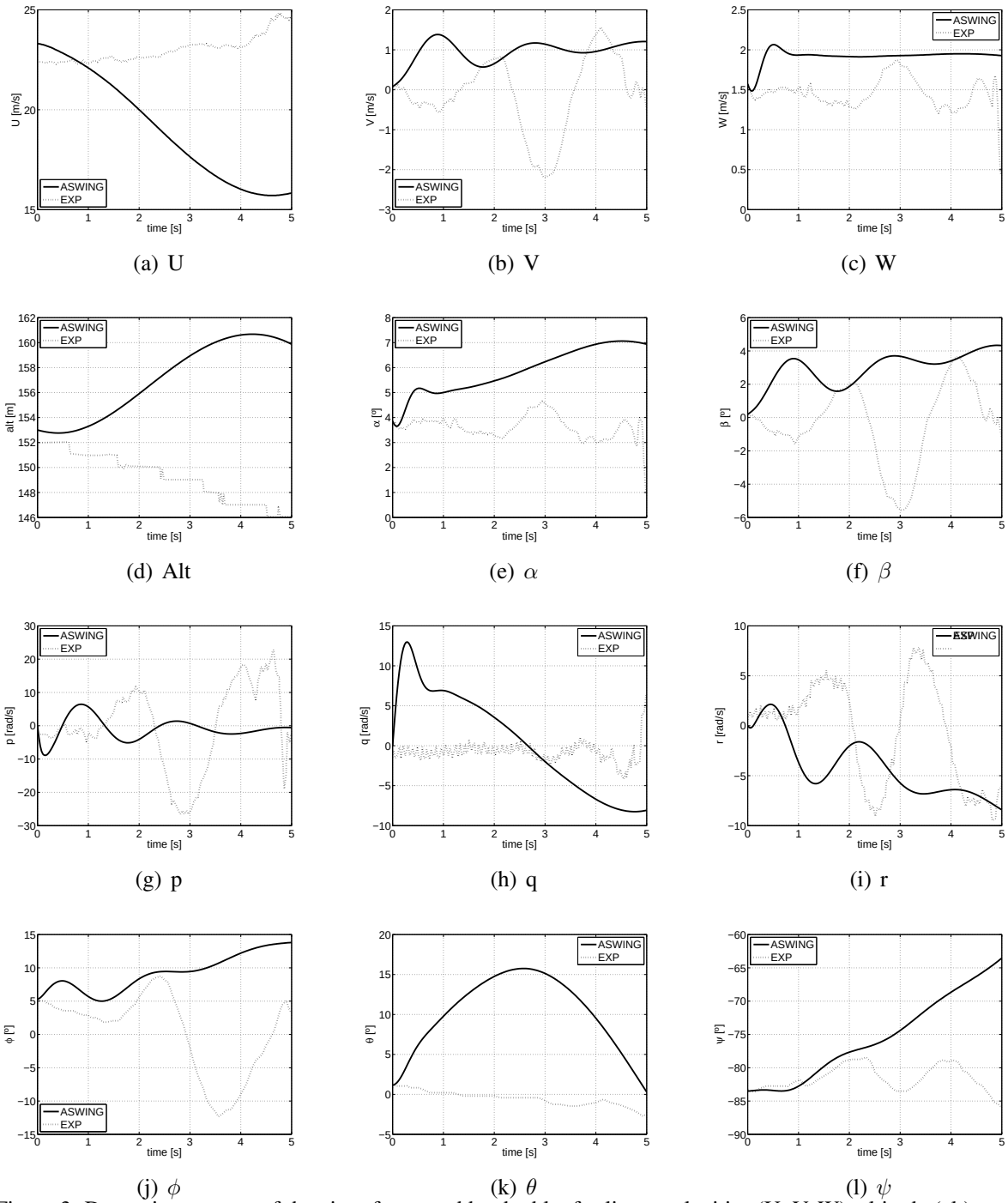

(a) U (b) V (c) W

(d) Alt (e) α (f) β

(g) p (h) q (i) r

(j) ϕ (k) θ (l) ψ

Figure 3: Dynamic response of the aircraft to a rudder doublet for linear velocities (U, V, W), altitude (alt), angle of attack (α), side-slip angle (β), angular velocities (p, q, r) and Euler angles (ϕ, θ, ψ).

perfectly the experimental results in general. Discrepancies are significant but experimental trends are in general captured by ASWING. The trends observed in ASWING results also allow the identification of the doublet effects in the angular rates. The deviation of ASWING results comparing to experimental data starts at the initial conditions, which has an effect on the subsequent time dependent results. Trimmed states were used to initiate the time domain analysis in ASWING with the already deformed aircraft state, which do not correspond to the initial conditions of the recorded experimental data. Even the trimmed state does not seem to be accurate enough to maintain the aircraft in a static state up to the time the disturbances are introduced. All these factors contribute to the discrepancies between the computational and

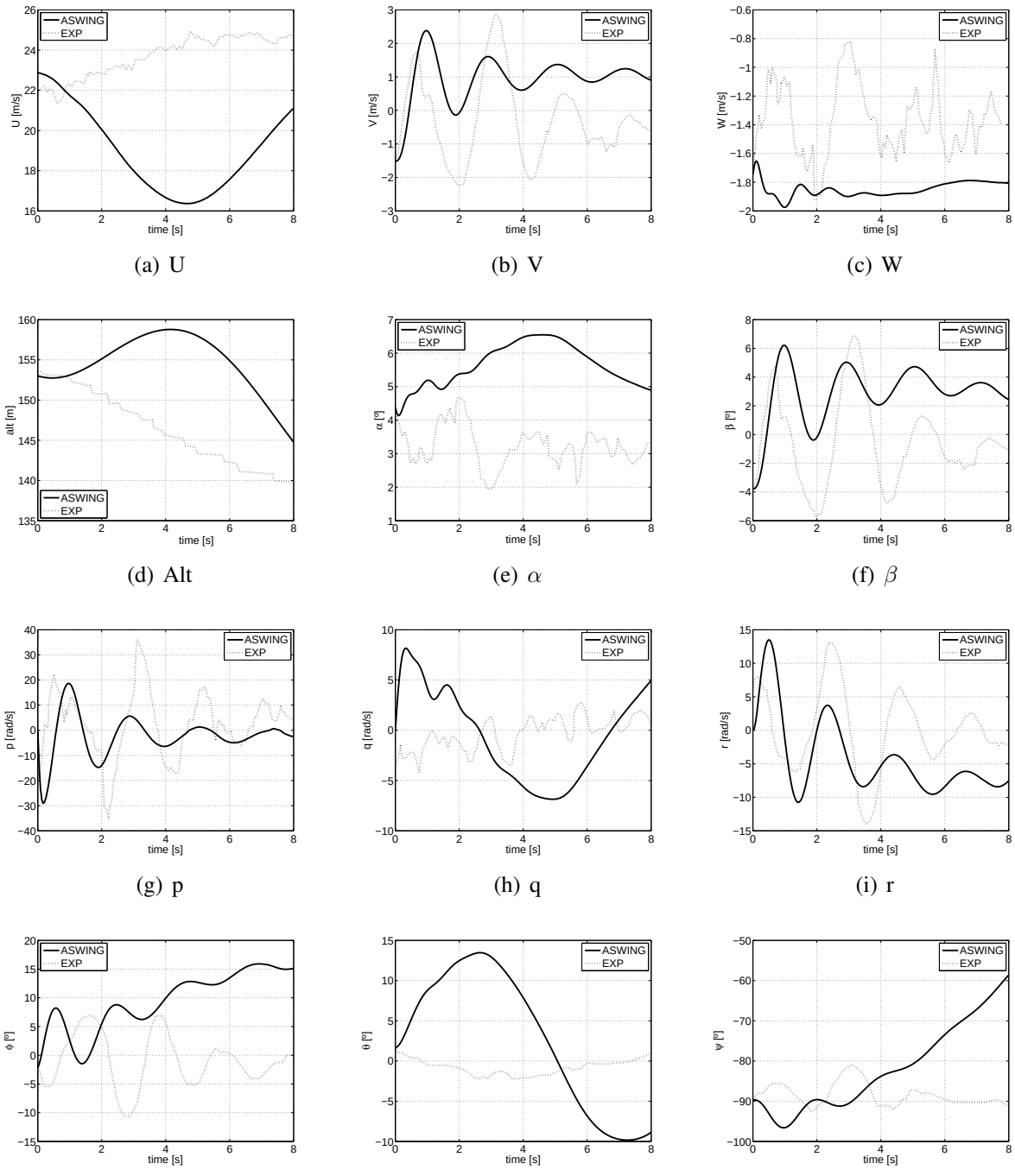

(a) U (b) V (c) W

(d) Alt (e) α (f) β

(g) p (h) q (i) r

(j) ϕ (k) θ (l) ψ

Figure 4: Dynamic response of the aircraft to an aileron doublet for linear velocities (U, V, W), altitude (alt), angle of attack (α), side-slip angle (β), angular velocities (p, q, r) and Euler angles (ϕ, θ, ψ).

experimental results. In addition to this, the used aerodynamic and propulsive models used in ASWING are of low fidelity which possibly will not model accurately the effects of control surfaces deflections and drag. This would lead to differences in linear and angular accelerations which, even if with small magnitude, would cause accumulated errors in velocity and angular rate components.

6 CONCLUDING REMARKS

The current paper describes a comparison between experimental and computational data from nonlinear analysis of a flexible wing aircraft. Results include stiffness, mass and inertia experimental determination used to build structural models through optimization in order to match the deformation and modal shapes and frequencies. The results from the analyses of the structural models showed good agreement with the experimental results. These structural models were then analyzed using a nonlinear aeroelastic analysis framework (ASWING) in order to simulate the aircraft behavior through a series of flight tests in which doublets were imposed on the control surfaces as disturbances. The comparison of results shows that the ASWING captures the major trends observed in the experimental data. The discrepancies in initial conditions used to start the simulations in ASWING as well as the low fidelity models used in this aeroelastic framework are two probable causes for the differences between the experimental and computational results. This work illustrates the importance of accurately modelling the multiple disciplines involved in flight simulation in order to obtain meaningful results in the aircraft design process.

ACKNOWLEDGMENTS

This work was carried out under a collaborative research program between Embraer S.A. and the University of Victoria, Canada. The MDO research team at IDMEC-LAETA-Instituto Superior Técnico was supported by the Fundação para a Ciência e Tecnologia under project no. UID/EMS/50022/2013. A.S. would like to acknowledge the NSERC Canada Research Chair and Discovery Research Grants.

7 REFERENCES

[1] Patil, M., Hodges, D. H., and Cesnik, C. E. S. (2001). Nonlinear aeroelasticity and flight dynamics of high-altitude-long-endurance aircraft. *Journal of Aircraft*, 38(1), 88–94.

[2] Patil, M. and Hodges, D. H. (2004). On the importance of aerodynamic and structural geometrical nonlinearities in aeroelastic behavior of high-aspect-ratio wings. *Journal of Fluids and Structures*, 19, 905–915.

[3] Tang, D. M. and Dowell, E. H. (2004). Effects of geometric structural nonlinearity on flutter and limit cycle oscillations of high-altitude-long-endurance aircraft. *Journal of Fluids and Structures*, 29, 291–306.

[4] Tang, D. M. and Dowell, E. H. (2001). Experimental and theoretical study on aeroelastic response of high-altitude-long-endurance aircraft. *AIAA Journal*, 39(8), 1430–1441.

[5] Tang, D. M. and Dowell, E. H. (2002). Experimental and theoretical study of gust response for high-altitude-long-endurance aircraft. *AIAA Journal*, 40(3), 419–429.

[6] Su, W. and Cesnik, C. E. S. (2011). Dynamic response of highly flexible flying wings. *AIAA Journal*, 49(2), 324–339.

[7] Patil, M. and Hodges, D. H. (2006). Flight dynamics of highly flexible flying wings. *Journal of Aircraft*, 43(6), 1790–1799.

[8] Shearer, C. M. and Cesnik, C. E. S. (2007). Nonlinear flight dynamics of very flexible wings. *Journal of Aircraft*, 44(5), 1528–1545.

[9] Van Schoor, M. C. and von Flotow, A. H. (2001). Aeroelastic characteristics of a highly flexible aircraft. *Journal of Aircraft*, 27(10), 901–908.

[10] Su, W. and Cesnik, C. E. S. (2010). Nonlinear aeroelasticity of a very flexible blended-wing-body aircraft. *Journal of Aircraft*, 47(5), 1539–1553.

[11] Drela, M. (1999). Integrated simulation model for preliminary aerodynamic, structural, and control-law design of aircraft. In *40th AIAA/ASME/ASCE/AHS/ASC Structures, Structural Dynamics, and Materials Conference*. Saint Louis, Missouri, USA. AIAA Paper 99-1394.

[12] Wang, Z., Chen, P., Liu, D., et al. (2010). Nonlinear-aerodynamic/nonlinear-structure interaction methodology for a high-altitude-long-endurance wing. *Journal of Aircraft*, 47(2), 556–566.

[13] Simpson, R. J. S., Palacios, R., and Murua, J. (2013). Induced-drag calculations in the unsteady vortex lattice method. *AIAA Journal*, 51(7), 1775–1779.

[14] Jones, J. R. and Cesnik, C. E. S. (2015). Preliminary flight test correlations of the X-HALE aeroelastic experiment. *The Aeronautical Journal*, 119(1217), 855–870.

[15] Suleman, A., Afonso, F., Vale, J., et al. (2017). Non-linear aeroelastic analysis in the time domain of high-aspect-ratio wings: Effect of chord and taper-ratio variation. *The Aeronautical Journal*, 121(1235), 16–29.

[16] Afonso, F., Leal, G., Vale, J., et al. (2016). A study on the effect of stiffness and geometric parameters on the nonlinear aeroelastic performance of high aspect-ratio wings. *Proc IMech E Part G: J Aerospace Engineering*. (In Press).

COPYRIGHT STATEMENT